11-10-2015

Spectroscopic Evidence of Nanodomains in THF/RTIL Mixtures: Spectroelectrochemical and Voltammetric Study of Nickel Porphyrins

Abderrahman Atifi
Marquette University

Michael D. Ryan
Marquette University, michael.ryan@marquette.edu

Accepted version. *Analytical Chemistry*, Vol. 87, No. 24 (November 10, 2015): 12245-12253. DOI.

Spectroscopic Evidence of Nanodomains in THF/RTIL Mixtures: Spectroelectrochemical and Voltammetric Study of Nickel Porphyrins

Abderrahman Atifi
Chemistry Department, Marquette University, Milwaukee, WI
Michael D. Ryan
Chemistry Department, Marquette University, Milwaukee, WI

Analytical Chemistry, Vol 87, No. 24 (November 10, 2015): pg. 12245-12253. DOI.

Abstract

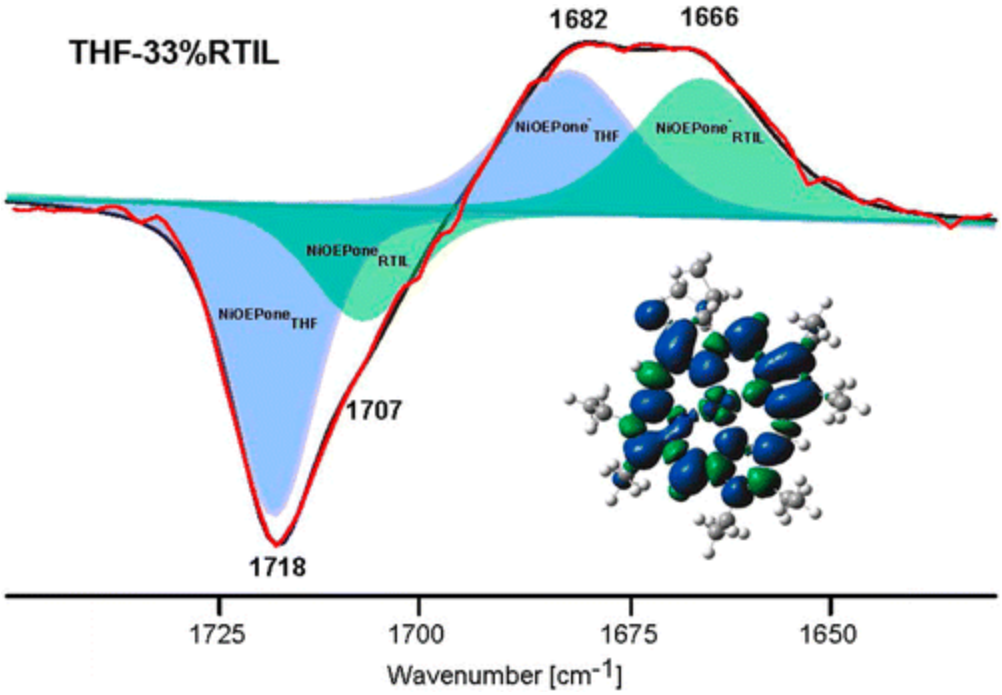

The presence and effect of RTIL nanodomains in molecular solvent/RTIL mixture were investigated by studying the spectroelectrochemistry and voltammetry of nickel octaethylporphyrin (Ni(OEP)) and nickel octaethylporphinone (Ni(OEPone)). Two oxidation and 2–3 reduction redox couples were observed, and the UV–visible spectra of all stable products in THF and RTIL mixtures were obtained. The $E°$ values for the reduction couples that were studied were linearly correlated with the Gutmann acceptor number, as well as the difference in the $E°$ values between the first two waves ($\Delta E_{12}° = |E_1° - E_2°|$). The $\Delta E_{12}°$ for the reduction was much more sensitive to the %RTIL in the mixture than the oxidation, indicating a strong interaction between the RTIL and the anion or dianion. The shifts in the $E°$ values were significantly different between Ni(OEP) and Ni(OEPone). For Ni(OEP), the $E_1°$ values were less sensitive to the %RTIL than were observed for Ni(OEPone). Variations in the diffusion coefficients of Ni(OEP) and Ni(OEPone) as a function of %RTIL were also investigated, and the results were interpreted in terms of RTIL nanodomains. To observe the effect of solvation on the metalloporphyrin, Ni(OEPone) was chosen because it contains a carbonyl group that can be easily observed in infrared spectroelectrochemistry. It was found that the ν_{CO} band was very sensitive to the solvent environment, and two carbonyl bands were observed for $Ni(OEPone)^-$ in mixed THF/RTIL solutions. The higher energy band was attributed to the reduced product in THF, and the lower energy band attributed to the reduced product in the RTIL nanophase. The second band could be observed with as little as 5% of the RTIL. No partitioning of $Ni(OEPone)^+$ into the RTIL nanodomain was observed. DFT calculations were

Analytical Chemistry, Vol 87, No. 24 (November 10, 2015): pg. 12245-12253. DOI.

carried out to characterize the product of the first reduction. These results provide strong direct evidence of the presence of nanodomains in molecular solvent/RTIL mixtures.

Because of their desirable physicochemical properties (wide electrochemical window, low volatility, low flammability and high thermal stability, etc.), room temperature ionic liquids (RTILs) have attracted considerable attention during the last decades as powerful solvents for electrochemical applications.[1] Room temperature ionic liquids are of interest to electrochemists because of their ability to stabilize charged species. This was shown most dramatically by the collapse of the two one-electron redox couples for dinitrobenzene into a single two-electron process.[2,3] Other workers have shown significant shifts in the $E°$ values, especially for dianionic species[4,5] in the presence of RTILs. Although RTILs have many useful properties, their high viscosity and price are a significant disadvantage. One of the aims of this work is to investigate whether mixed molecular/RTIL solutions can gain many of the advantages of RTILs while minimizing these disadvantages.

In mixed molecular/RTIL solvents, aggregates can form that can lead to nanodomains of RTILs in the molecular solvents.[6] The formation of these nanodomains can lead to additional stabilization of the electrogenerated species. Li et al.[7] studied the micropolarity and aggregation behavior of RTILs with organic solvents. For solvents with a moderate dielectric constant like acetonitrile, the polarity parameter, π*, was linearly related to the volume fraction of the RTIL. For low dielectric constant molecular solvents, solutes can induce preferential solvation[8] or the formation of aggregates in the absence of the probe.[9,10]

Most studies on the effect of RTILs on the redox potentials of substrates have focused on the formation of anions by electroreduction.[5,11,12] Much less work has been dedicated to the study of the formation of positively charged species with RTILs.[1] For instance, in their work on the reactivity of organic radical cations in different RTILs, Lagrost et al. have reported no significant effect on oxidation potentials, but only monocations were formed.[13] This was not unexpected in that minimal effects were also observed for monoanions.

Analytical Chemistry, Vol 87, No. 24 (November 10, 2015): pg. 12245-12253. DOI.

In this study, the voltammetry and spectroelectrochemistry (SEC) of Ni(OEP) (OEP = octaethylporphyrin) and Ni(OEPone) (OEPone = octaethylporphinone) were examined in mixtures of THF and RTILs. The latter compound is useful for vibrational studies because of the strong carbonyl vibration in the infrared region. The voltammetry of both complexes exhibited at least two reversible one-electron reduction and three one-electron oxidation redox couples.[14-18] Lexa et al.[16] formulated the first reduction product to be $Ni^{I}(OEP)^{-}$ using UV–visible and EPR spectroscopies.

$$Ni^{II}(OEP) + e^{-} \rightarrow Ni^{I}(OEP)^{-} \quad (1)$$

This result was confirmed by Nahor et al.,[19] though they did observe that some nickel porphyrins could form π-anion radicals. These factors were studied in more detail by Kadish et al.[14,15] The product of the second redox process has not been studied in detail.

Three redox couples have been observed for the oxidation. The first two were reversible, whereas the third redox couple's reversibility depended upon the macrocycle. The product of the first redox couple led to a π-cation radical ($Ni^{II}(OEP^{+\bullet})$), as shown by UV–visible, EPR and resonance Raman spectroscopy.[20-22]

$$Ni^{II}(OEP) \rightarrow Ni^{II}(OEP^{\bullet})^{+} + e^{-} \quad (2)$$

Scheidt and co-workers have shown that mixed valence dimers, $[(Ni(OEP)_2]^{+}$, can also be formed.[23,24] The mixed dimer can be reduced/oxidized at about the same potential as the Ni(OEP) oxidation couple.[23] The second redox couple leads to further oxidation of the porphyrin to the dication:

$$Ni^{II}(OEP^{\bullet})^{+} \rightarrow Ni^{II}(OEP)^{2+} + e^{-} \quad (3)$$

A weak broad visible spectrum with a Soret band at 330 nm was observed.[22] This spectrum was similar to the zinc and magnesium dications.[25] A third oxidation redox couple was observed by Kadish et al.,[15] which was deduced to be a Ni(III) porphyrin species. This redox couple was irreversible for Ni(OEP) due to an EC mechanism, but reversible electron transfers were observed for other porphyrin structures.

There have been relatively few electrochemical studies of metalloporphyrins in RTILs.[26-28] Compton and Laszo[28] studied the

Analytical Chemistry, Vol 87, No. 24 (November 10, 2015): pg. 12245-12253. DOI.

voltammetry of hemin in mixed molecular/RTIL solutions (pyridine/*N*-methyl imidazole and $BMImPF_6$/$OMImPF_6$. BMIm: 1-butyl-3-methyl imidazolium. OMIm: 1-octyl-3-methyl imidazolium.). Hemin has little solubility in these ionic liquids, and was studied as an adsorbed layer on a gold electrode in contact with $BMImPF_6$ or $OMImPF_6$. Reversible redox couples for hemin were observed in both cases.

The aim of this work will be to evaluate the effect of RTILs on the oxidation and reduction potentials of Ni(OEP) and Ni(OEPone) to assess the differences in the ability of the RTILs to interact with cationic and anionic substrates. In addition, FTIR spectroelectrochemistry was carried out on Ni(OEPone) to study the partitioning of metalloporphyrins between the THF and RTIL nanodomains.

Experimental Section

Instruments

Cyclic voltammetry (CV) was carried out using a Model 600D Series Electrochemical Analyzer/Workstation (CHI Version 12.06). Platinum working electrodes (diameter: 1.6 mm or 10 μm), platinum wire auxiliary and Ag/0.10 M $AgNO_3$/CH_3CN reference were used in the voltammetric cell. Spectroelectrochemical (SEC) experiments were made with a low-volume thin layer quartz glass cell purchased from BAS Inc. A platinum mesh was used as the working electrode and a platinum wire was used as the auxiliary electrode. Potentials were measured relative to the $Ag/AgNO_3$ (in CH_3CN) reference electrode. The UV–visible spectra were recorded on a HP 8452A diode array spectrophotometer. A *Specac* spectroelectrochemical transmission cell (Specac Ltd., Kent, UK) was used to carry out the FTIR SEC experiments. The cell was composed of two CaF_2 windows separated by a 100 μm sample layer, where gold grid working and auxiliary electrodes and a silver reference electrode were photolithographically imprinted on the surface of the front window in contact with the sample. The infrared spectra were obtained using 64 scans and 2 cm^{-1} resolution, recorded with a Thermo Nicolet-FTIR spectrophotometer (Model 670 Nexus) with a MCT detector. ^{31}P NMR measurements were performed using a Varian 400 MHz FT spectrometer. The viscosities of

Analytical Chemistry, Vol 87, No. 24 (November 10, 2015): pg. 12245-12253. DOI.

the solutions were measured using a Brookfield DV2T viscometer, and the temperature was controlled with a water bath.

Chemicals

Nickel(II) octaethylporphyrin (NiOEP), tetrabutylammonium perchlorate (TBAP), ethyldimethylpropylammonium bis(trifluoromethylsulfonyl)imide ($AmNTf_2$) and 1-butyl-3-methylimidazolium hexafluorophosphate ($BMImPF_6$) were purchased from Sigma-Aldrich Chemical Co. and used as received. The ligand, H_2OEPone, was synthesized by literature procedures.[29] Anhydrous tetrahydrofuran (THF) was purchased from Sigma-Aldrich Chemical Co. and refluxed in the presence of sodium and benzophenone under nitrogen until the solution was a deep blue. Activated alumina was obtained from EMD (chromatographic grade, 80–200 mesh). No additional pretreatment was done on the alumina. To form Ni(OEPone), nickel(II) acetate tetrahydrate (98%, Aldrich) was refluxed with H_2OEPone in $CHCl_3$/MeOH (20/10 mL) for 1 h. The resulting solution was cooled to room temperature and washed 3 times with 300 mL of water. After the solvent was removed with a rotatory evaporator, the crude product was purified using a 12 in. alumina column (diameter = 0.75 in.) and the elution was initiated with chloroform. The product was characterized by UV–visible and IR spectroscopy.

Computational Methods

The Gutmann acceptor numbers (AN) were calculated using the NMR procedure of Schmeisser et al.[30] This procedure was developed to determine AN in RTILs. The ^{31}P chemical shift of Et_3PO was measured at a series of concentrations and extrapolated to infinite dilution. From the chemical shift, the acceptor number was calculated using an empirical equation. Deconvolution of the difference FTIR spectra was carried using Grams/32 AI software (Galactic Industries, Salem, NH) to identify individual bands. Electronic structure and vibrational spectral calculations were carried out with the Gaussian 09 suite of programs[31] using the m06 DFT functional and the TZVP basis set for all elements except for nickel. The Wachters' basis set was used for nickel.[32] All calculations converged using the tight optimization criteria. A scale factor of 0.94 was used for the m06 calculation of IR spectra, based on the empirical fit for a series of metalloporphinones.[29]

Analytical Chemistry, Vol 87, No. 24 (November 10, 2015): pg. 12245-12253. DOI.

Procedure

Cyclic voltammetric experiments were carried out under an argon atmosphere. The formal potentials ($E°$ values) were measured from the average of the E_{pc} and E_{pa} values for each redox couple. All $E°$ values should be considered to be formal potentials, which may deviate from the thermodynamic $E°$ value due factors such as the ionic strength and diffusion coefficient ratios. All solutions were prepared and placed into the spectroelectrochemical cell in the glovebox under an argon environment. UV–visible and FTIR spectroelectrochemical experiments were carried out using two methods depending upon the solution. For UV–visible spectra in molecular solvents, a slow cyclic scan of the potential was sufficient to ensure complete electrolysis at each potential. For RTIL solutions (visible) and for FTIR spectroelectrochemistry (all solutions), the potential step method was used to obtain the spectra. The potentials were chosen to be sufficiently negative (for reductions) or positive (for oxidations) to ensure complete electrolysis. Water was removed from the RTIL by passing N_2 over the solvent heated at 70 °C. The amount of water in the RTIL was measured by monitoring the stripping peak on a gold electrode due to water.[3,33] After this treatment, the water stripping peak completely disappeared. Solutions of THF were prepared with 0.10 M TBAP as the supporting electrolyte.

Results and discussion

Cyclic Voltammetry and Visible Spectroelectrochemistry of Ni(OEP)

The cyclic voltammetry of Ni(OEP) in pure THF is shown in Figure 1 (black trace). Four reversible redox couples were observed under the conditions of the experiment: two reversible reduction couples at −1.74 and −2.47 V, and two oxidation couples at +0.54 and +0.79 V. The product of the second reduction was not completely stable on the voltammetric time scale, and an additional oxidation peak (Peak A, E_{pa} = −0.88 V in THF) was observed on the reverse scan. If the potential was reversed at −2.0 V, this new oxidation peak was not observed. Such peaks, which may be due to a decomposition product, were reported previously by Kadish et al. for nickel porphyrins

Analytical Chemistry, Vol 87, No. 24 (November 10, 2015): pg. 12245-12253. DOI.

reductions.[15] The study of this reaction is beyond the scope of the present investigation, but the second redox couple was chemically reversible enough to measure the $E_2°$ for the reduction. The semiderivative analysis of the two reduction and two oxidation redox couples showed that each couple was a one-electron process.

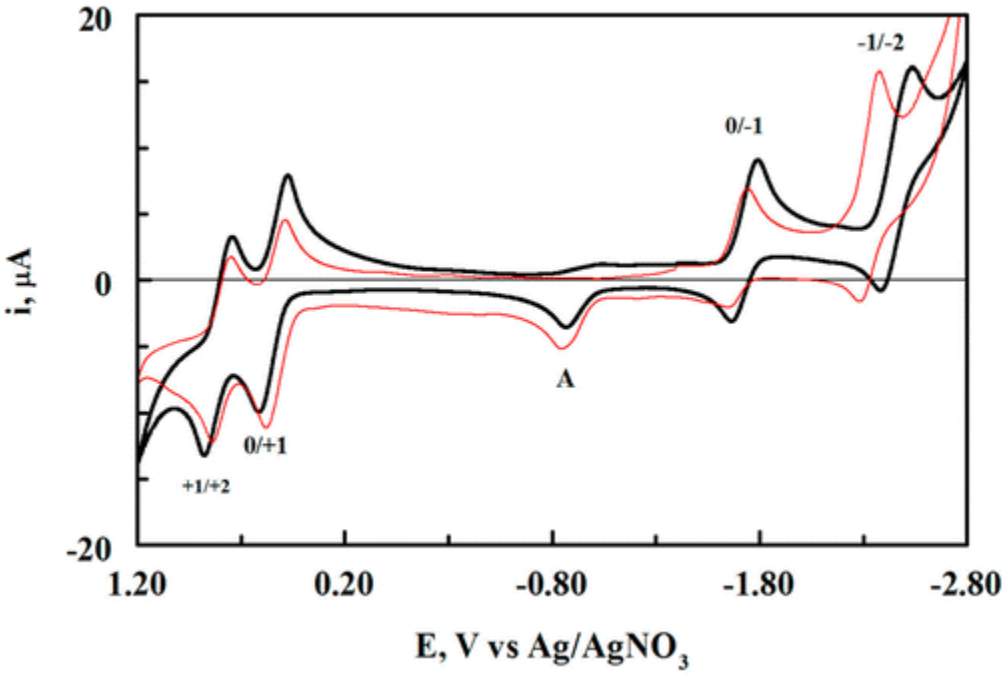

Figure 1. Cyclic voltammetry of 2.0 mM Ni(OEP) in THF/0.10 M TBAP with 5% $AmNTf_2$ (red line) and without $AmNTf_2$ (black line). Scan rate = 100 mV/s. $E_{initial}$ = −1.40 V, initial scan is negative. Working electrode: Pt (diameter = 1.6 mm). Auxiliary electrode: Pt.

The UV–visible spectroelectrochemistry was carried out for the first reduction and the two oxidation processes in THF. The first reduction product ($Ni(OEP)^-$) gave the same spectrum as previously reported.[16,34] This species has been previously described by Lexa et al.[16] as a Ni(I) complex. The reoxidation scan allowed for the complete recovery of the Ni(OEP) spectrum. The instability of the product of the second reduction redox couple precluded the acquisition of a spectrum for the two electron product. During the oxidation of Ni(OEP) in THF, the Soret band decreased significantly in molar absorptivity, which was consistent with reports by previous workers (Figure S1).[21,22] Although isosbestic points were observed from the initial spectrum to +0.74 V, the isosbestic points were lost at more positive potentials, indicating the formation of a third spectroscopic species. On the basis of previous

Analytical Chemistry, Vol 87, No. 24 (November 10, 2015): pg. 12245-12253. DOI.

work by Scheidt et al.,[23,24] the spectra in this potential range are probably a combination of Ni(OEP), $Ni(OEP)^+$ and the oxidized dimer, $[Ni(OEP)]_2^+$. The complete oxidation of Ni(OEP) yielded a spectrum for $Ni(OEP)^+$ that was consistent with the spectrum for $Ni(OEP)^+$ in methylene chloride.[35] Further oxidation of $Ni(OEP)^+$ led to the formation of $Ni(OEP)^{2+}$ (Figure S1C). The broad dication spectrum was consistent with previous reports, though some $Ni(OEP)^+$ could still be observed in the final spectrum. Although evidence of the cation dimer was observed in the THF electrolysis, there was no evidence of this species in the spectroelectrochemistry of Ni(OEP) in methylene chloride (Figure S2).

Cyclic Voltammetry and Spectroelectrochemistry of Ni(OEP) in THF/RTIL Mixtures

The cyclic voltammetry of Ni(OEP) in mixtures of THF/$AmNTf_2$ is shown in Figure 1 (red trace). With the addition of $AmNTf_2$, all four redox couples can still be observed. In the presence of $AmNTf_2$, the two oxidation $E°$ values were shifted to less positive potentials, but larger shifts in the positive direction were observed for the reduction redox couples, especially the second one. The shifts in the two reduction and two oxidation $E°$ values as a function of the %$AmNTf_2$ are summarized in Table S1. A more direct measure of the ability of the mixtures to solvate the electroactive species is the Gutmann acceptor number (AN). The Gutmann AN were measured as described in the Experimental Section using NMR. The relationship between the Gutmann AN and the %RTIL was nonlinear. The two oxidation $E°$ values were shifted to more negative potentials with the addition of the RTILs. The slopes of the trend lines for the two oxidation $E°$ values versus the Gutmann AN were very small (2.92 mV/AN for the 0/+1 redox couple and 2.06 mV/AN for +1/+2 redox couple), and not well correlated with the Gutmann AN (R^2 = 0.71 and 0.50 for the 0/+1 and +1/+2 redox couples, respectively). The two reduction processes were shifted to more positive potentials, and were better correlated with the Gutmann AN as expected for the formation of anions. The Gutmann AN is a measure of the Lewis acidity of the solvent, which will stabilize the more basic species (e.g., $Ni(P)^-$ and $Ni(P)^{2-}$), than more acidic species (e.g., $Ni(P)^+$ and $Ni(P)^{2+}$). The slope for the 0/−1 redox couple was 6 mV/AN (R^2 = 0.94), whereas the slope for the −1/−2 redox couple was 21 mV/AN (R^2 = 0.99; only the first redox couple could be observed

Analytical Chemistry, Vol 87, No. 24 (November 10, 2015): pg. 12245-12253. DOI.

for Ni(OEP) in $BMImPF_6$ due to a smaller electrochemical window in that RTIL). For the first reduction process, the shifts in the $E°$ values followed a single trend line, which depended only on the Gutmann AN, rather than the identity of the RTIL. Much larger slopes were observed for the reduction redox couples, as compared to the oxidation couples. The quantitative values of the individual slopes are not meaningful because the shifts are confounded with shifts in the reference system. The relative values between individual redox couples and molecular systems, though, indicate the relative sensitivity of the redox potential to changes in the %RTIL.

To eliminate issues with the reference system, the difference between the first and second redox couples ($\Delta E_{12}° = |E_1° - E_2°|$) as a function of the Gutmann acceptor number was calculated.[5] The use of potential differences thus reduces these uncertainties. The results are shown in Figure 2 for both RTILs (the second reduction redox couple was not observable for $BMImPF_6$). For $\Delta E_{12,red}°$, the difference decreased linearly (slope = −12.5 mV/AN, R^2 = 0.99) as the Gutmann acceptor number increased. This result was consistent with significantly higher solvation of the dianion by the RTIL as compared with the monoanion. On the other hand, the $\Delta E_{12,ox}°$ had a positive slope as expected showing that the dication was less stabilized in higher Gutmann acceptor solution than the monocation. This is to be expected for cationic species. The slope though was quite small (1.3 mV/AN) and less well correlated (R^2 = 0.79) with the Gutmann AN.

Analytical Chemistry, Vol 87, No. 24 (November 10, 2015): pg. 12245-12253. DOI.

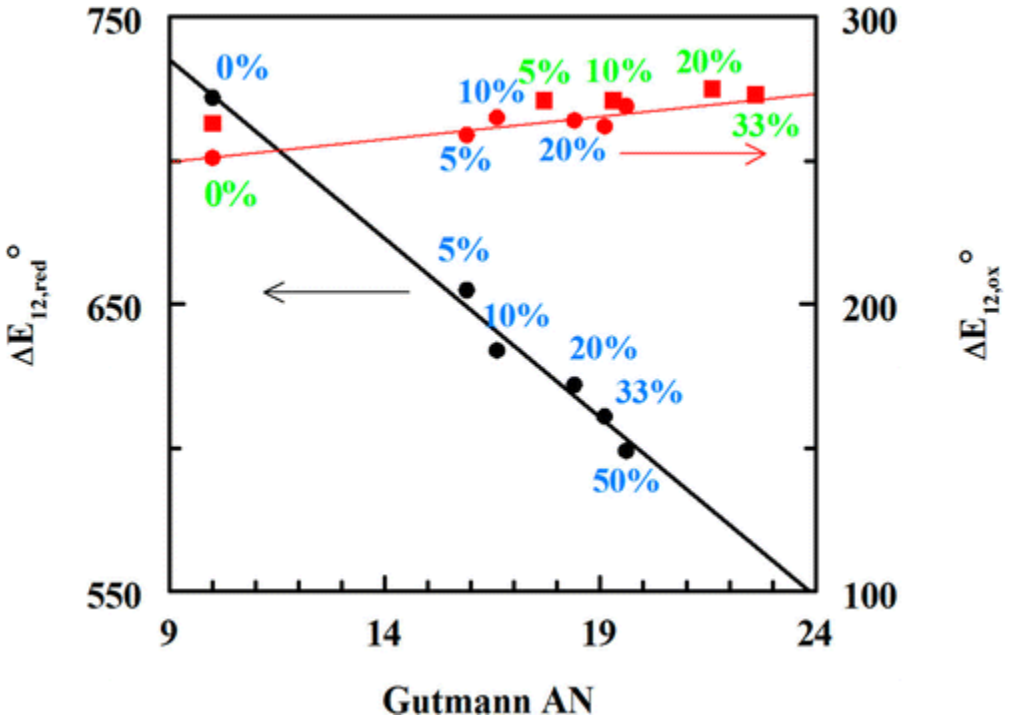

Figure 2. Plot of the $\Delta E_{12}°$ values for the reduction (black symbols/line) and oxidation (red symbols/line) for the voltammetry of Ni(OEP) in THF/RTIL mixtures. The %RTIL in the THF/RTIL mixtures is given on the graph. (Blue: $AmNTf_2$ mixtures (33% and 50% omitted on for the oxidation values for clarity. Green: $BMImPF_6$ mixtures.)

As RTILs were added to the THF solution, the viscosity of the solution increased. The increase in viscosity should decrease the diffusion coefficient by the Stokes–Einstein equation:

$$D = \frac{k_B T}{6\pi\eta r} \quad (1)$$

The ratio of the diffusion coefficient in the mixed solution ($D_{mixture}$) to the diffusion coefficient in THF (D_{THF}) can be calculated from the semiintegral which reduces the effect of quasi-reversibility and uncompensated resistance. From the Stokes–Einstein equation, the ratio of the diffusion coefficients should be inversely proportional to the viscosity ratios:

$$\frac{D_{mixture}}{D_{THF}} = \frac{\eta_{THF}}{\eta_{mixture}} \quad (2)$$

k_B = Boltzmann constant, T = temperature, η = viscosity and r = molecular radius.

Analytical Chemistry, Vol 87, No. 24 (November 10, 2015): pg. 12245-12253. DOI.

The results are shown in Figure 3. The viscosity ratios are also plotted as a line on the graph. The viscosity ratios for both $AmNTf_2$ and $BMImPF_6$ were nearly identical for solutions that were mostly molecular solvents (even at 50% RTIL, the mole fraction of RTIL was around 0.22). Up to about 50% RTIL, the diffusion coefficient ratios were larger than the viscosity ratio, but trended to the same values for high concentration of the RTIL. This indicates that the diffusion was faster than predicted by the Stokes–Einstein equation for mixtures where the %RTIL was less than 50%. It has been previously shown that the Stokes–Einstein relationship has been followed in most cases for the diffusion of electroactive materials in RTILs[36-38] and molecular solvents.[39,40] Unlike the viscosity ratio that followed an exponential relationship, the diffusion coefficient ratio decreased linearly with %RTIL. As with the viscosity ratios, the diffusion coefficient ratios depended on the %RTIL and not the identity of the RTIL. These results are consistent with the presence of molecular solvent and RTIL domains within the mixed solvent systems and that the electroactive species diffuses mostly within the molecular solvent region. The dashed line in the figure is a linear fit to the diffusion ratio data.

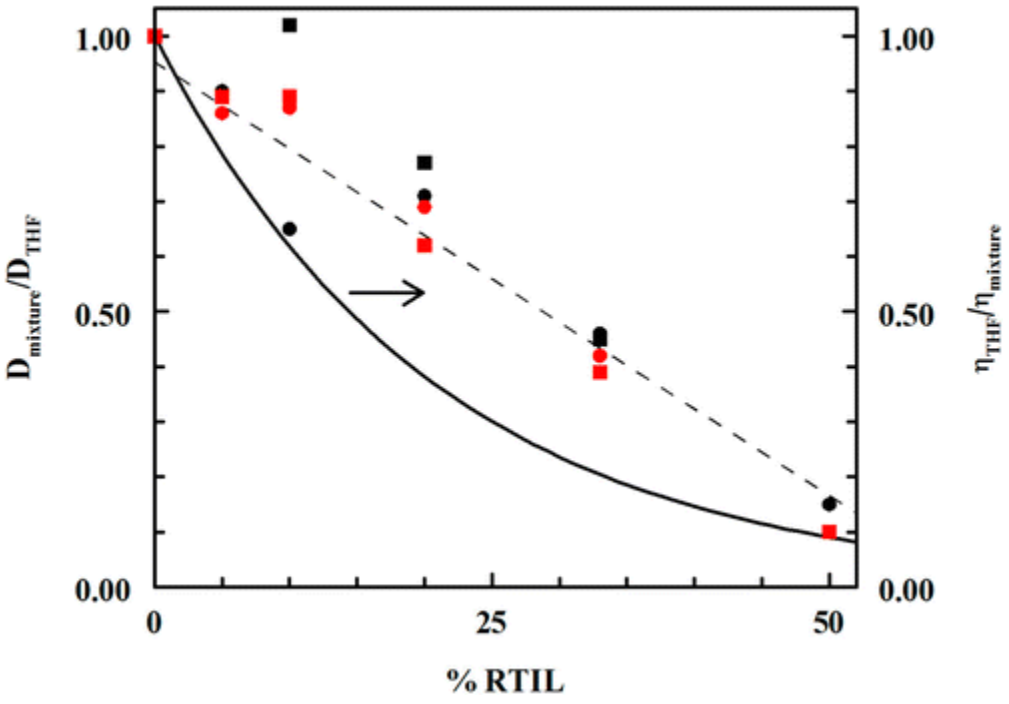

Figure 3. Plot of the viscosity ratio/diffusion coefficient ratio as a function of %RTIL. The viscosity and diffusion coefficients are normalized to the values in THF. Line is the viscosity ratio ($\eta_{THF}/\eta_{mixture}$). Diffusion coefficient ratios: Ni(OEP) first reduction couple

Analytical Chemistry, Vol 87, No. 24 (November 10, 2015): pg. 12245-12253. DOI.

($AmNTf_2$, black •; $BMImPF_6$, red •), Ni(OEPone) first reduction couple ($AmNTf_2$, black ■; $BMImPF_6$, red ■).

The visible spectroelectrochemistry of Ni(OEP) was carried out in THF and THF/$AmNTf_2$ mixtures. No changes were observed in the visible spectra of Ni(OEP) in THF or mixed solvents (Figure S3). Small blue shifts were observed for the two major bands in $Ni(OEP)^-$ when $AmNTf_2$ was added to the solution. The Soret band shifted from 406 to 404 nm, whereas the Q-band shifted from 546 to 542 nm (Figure S3). Overall, the spectrum was consistent with a Ni(I) complex in the presence or absence of the RTIL, but small changes were observed due to the presence of the RTIL. The oxidation of Ni(OEP) in pure THF and THF/10% $BMImPF_6$ was quite similar. No noticeable shifts were observed in the Soret band for the cation and dication. The cation dimer appeared to be more stable than in pure THF, making it more difficult to see $Ni(OEP)^+$ before the second oxidation occurs.

Cyclic Voltammetry and Spectroelectrochemistry of Nickel Octaethylporphinone (Ni(OEPone))

To investigate the interactions between the RTIL and the electroactive material (and its redox products), the electrochemistry and spectroelectrochemistry of Ni(OEPone) were investigated. Visible spectroelectrochemistry of $Ni(OEP)^-$ showed some spectral shifts due to the RTIL, but these shifts are difficult to interpret on a molecular level. On the other hand, the porphinone ligand has a carbonyl group that can be readily observed using infrared spectroelectrochemistry, and this group creates a polar moiety on the ring that may interact strongly with the RTIL cation. The cyclic voltammetry of Ni(OEPone) is shown in Figure 4. With this complex, three reduction and two oxidation redox couples were observed, and they were all chemically reversible. The $E_1°$ of Ni(OEPone) was shifted by 163 mV to more positive potentials in THF as compared to Ni(OEP). Similar shifts was observed by Stolzenberg and Stershic.[34] Shifts of 94 mV (for ZnOEP/ZnOEPone) and 367 mV (for MnOEP/MnOEPone) have been observed for reductions that have been assigned to the formation of π-anion radicals. Smaller shifts were observed for FeOEP/FeOEPone (30 mV) and CoOEP/CoOEPone (20 mV) where M(I) species were formed. Thus, the change in the ring structure might affect the electron structure of the $Ni(P)^-$ product. The second reduction $E°$ of Ni(OEPone) was 210 mV positive of the Ni(OEP) couple. Both oxidation $E°$ values

Analytical Chemistry, Vol 87, No. 24 (November 10, 2015): pg. 12245-12253. DOI.

of Ni(OEPone) were shifted to less positive potentials, as compared with Ni(OEP); the first *E*° by 50 mV and the second *E*° by 75 mV. This compares with a 20 and 30 mV shift of the *E*° in acetonitrile and methylene chloride, respectively, and a 60 (acetonitrile) and 100 mV (methylene chloride) shift of the E_2° value.[18] The third reduction of Ni(OEPone) has not been previously reported.

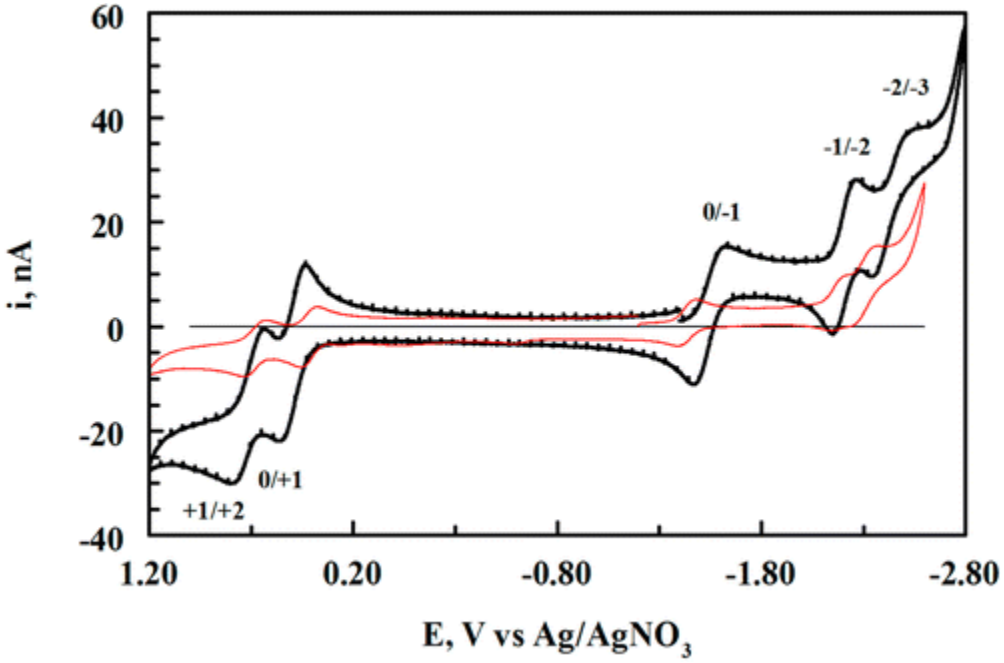

Figure 4. Cyclic voltammetry of 2.0 mM Ni(OEPone) in THF/0.10 M TBAP with 33% $AmNTf_2$ (red line) and without $AmNTf_2$ (black line). THF solution: scan rate = 100 mV/s. $E_{initial}$ = −1.40 V for THF, initial scan is negative. 33% $AmNTf_2$ solution: scan rate = 10 V/s. $E_{initial}$ = −1.20 V, initial scan is negative. Working electrode: Pt (*d* = 10 μm). Auxiliary electrode: Pt.

With the addition of $AmNTf_2$, the reduction peaks shifted to more positive potentials whereas the oxidation peaks shifted to less positive potentials (Figure 4). The shifts in potentials as a function of Gutmann AN are shown in Table 1. Although the potentials were linearly correlated with the Gutmann AN as with Ni(OEP), there were important differences. The slope of the first reduction process for Ni(OEPone) (15.3 mV/AN, R^2 = 0.97) was more than 2 times as large as the slope observed for Ni(OEP) (6.0 mV/AN). The second redox couple, by contrast, was less sensitive to the Gutmann AN (3.4 mV/AN, R^2 = 0.84), whereas the slope of the third redox process was one-third smaller than the slope for the first couple (11.4 mV/AN, R^2 =

Analytical Chemistry, Vol 87, No. 24 (November 10, 2015): pg. 12245-12253. DOI.

0.96). As was observed for Ni(OEP), a smaller dependence was observed for the oxidation process. The slope for the $E_1°$ value was 9.4 mV/AN (R^2 = 0.95) which is significantly larger than the slope for Ni(OEP) (2.9 mV/AN). The slope for the $E_2°$ value (2.8 mV/AN; R^2 = 0.67) was similar to that for Ni(OEP) (2.1 mV/AN) for the second redox couple. Because of these shifts, the $\Delta E_{12}°$ for the reduction increased as the Gutmann AN increased (12 mV/AN, R^2 = 0.98). This was the opposite of the results for Ni(OEP), where the two redox processes grew closer together. These reflected the significant interactions between the RTIL and Ni(OEPone)$^-$ as compared to Ni(OEPone). The insensitivity of the $E_2°$ value to the concentration of the RTIL indicated that the monoanion and dianion interacted equally strongly with the RTIL nanodomains. The $\Delta E_{23}°$ values returned to the normal trend, where the two redox couples moved closer together as the Gutmann AN increased (slope = 8.3 mV/AN; R^2 = 0.94). The $\Delta E_{12}°$ values for the oxidation of Ni(OEPone) were qualitatively different from those for Ni(OEP), where the two oxidation redox couples grew apart as the Gutmann AN increased (slope = 6.6 mV/AN, R^2 = 0.83). This result may not be statistically significant because of the small number of data points and the low value of R^2.

Table 1. Cyclic Voltammetry of Ni(OEPone) in THF/$AmNTf_2$ Mixtures

%$AmNTf_2$	reduction $E_1°$[a]	$E_2°$[a]	$E_3°$[a]	oxidation $E_1°$[a]	$E_1°$[a]	acceptor number
0	−1.549	−2.209	−2.415	0.492	0.718	10.0
5.0	−1.523	−2.204		0.456	0.717	16.0
10	−1.492	−2.195	−2.364	0.419	0.715	16.6
20	−1.452	−2.177	−2.332	0.410	0.704	18.4
33	−1.437	−2.174	−2.306	0.411	0.682	19.1
50	−1.441	−2.185	−2.303			19.6

[a]V vs $Ag/AgNO_3$ in CH_3CN.

The visible spectroelectrochemical reduction of Ni(OEPone) in THF (first redox couple) is shown in Figure 5. Upon reduction, the Soret band was significantly bleached with new Soret bands at 418 and 467 nm. In addition, a broad weak band was observed between 600 and 750 nm. Bleaching of the Soret band and a broad band between 600 and 750 nm are frequently an indication of a π-anion radical.[19] There were similarities and differences between Ni(OEPone)$^-$ and Zn(OEPone)$^-$, which is known to form a π-anion radical species. Although Zn(OEPone)$^-$ has a broad band at 452 nm, the Soret band was not split as in the nickel complex. Reduction of both complexes led

Analytical Chemistry, Vol 87, No. 24 (November 10, 2015): pg. 12245-12253. DOI.

to bleaching of the 621 nm band. Although there were characteristics in the UV–visible spectroelectrochemistry of both metal and ring reduction for Ni(OEPone), the UV-spectra was more consistent with a π-anion radical species. The visible spectroelectrochemistry of Ni(OEPone) in THF/33% $AmNTf_2$ was quite similar to pure THF. The only significant differences were the blue shifts in the split Soret bands from 418 to 406 nm, and from 468 to 463 nm. Blue shifts were also observed for Ni(OEP) in THF/RTIL mixtures, though greater shifts were observed for $Ni(OEPone)^-$ (12 and 5 nm) than for $Ni(OEP)^-$ (2 nm).

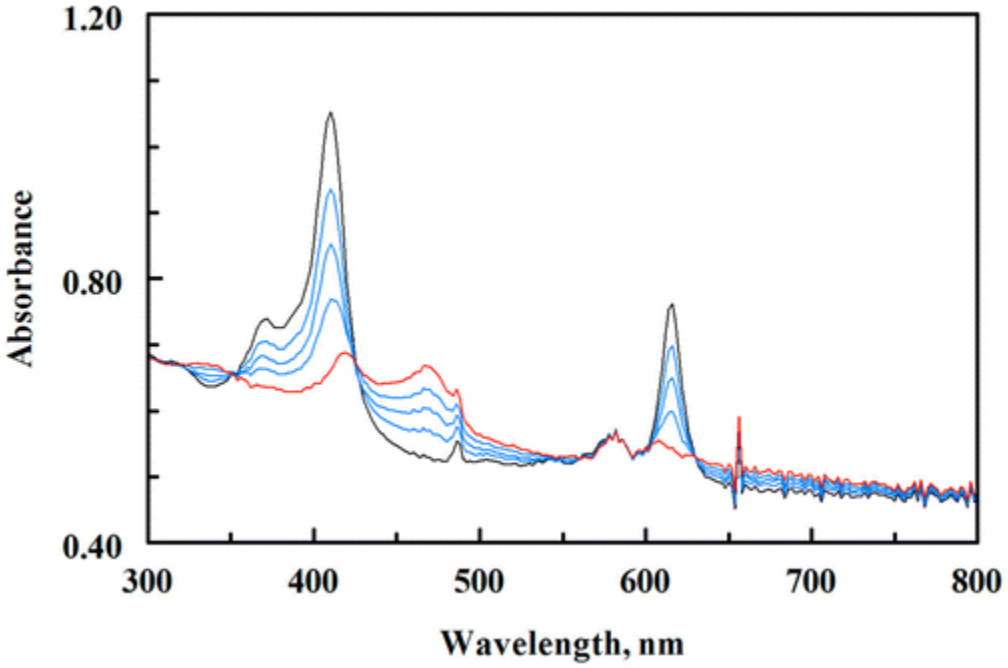

Figure 5. Spectroelectrochemical reduction of Ni(OEPone) to $Ni(OEPone)^-$ in THF. Black line: initial Ni(OEPone) spectrum. Red line: $Ni(OEPone)^-$ spectrum after removal of residual Ni(OEPone). Blue lines: intermediate spectra at 25, 60, and 171 s. Potential stepped from −1.0 to −1.8 V vs $Ag/AgNO_3$ (CH_3CN) for THF.

In the FTIR spectrum, the carbonyl band, ν_{CO}, for Ni(OEPone) was observed at 1718 cm^{-1} in THF, but was downshifted by about 4 cm^{-1} when the substrate was dissolved in $AmNTf_2$. Thus, the interaction between the ionic solvent and Ni(OEPone) has a small but measurable effect on the carbonyl band. The FTIR spectroelectrochemistry of Ni(OEPone) was carried out to see if similar shifts can be observed in the $Ni(OEPone)^-$ product. The FTIR difference spectrum is shown in Figure 6 (red curve) for the first reduction of Ni(OEPone) in THF. The ν_{CO} at the 1718 cm^{-1} band for the carbonyl

Analytical Chemistry, Vol 87, No. 24 (November 10, 2015): pg. 12245-12253. DOI.

disappeared whereas new bands at 1682, 1608, 1573, and 1541 cm^{-1} appeared. The band at 1682 cm^{-1} is consistent the carbonyl band of $Ni(OEPone)^{-}$.[29,41,42] The additional bands were typical of reduced metalloporphinones.[29,41,42] Previous work has shown that it is difficult to distinguish metal vs ring reduction of metalloporphinones based on the ν_{CO} shifts.[29] Differences in the ν_{CO} bands for π-anion radicals ($Zn(OEPone)^{-}$: 1662 cm^{-1}. $Mn(OEPone)^{-}$, 1657 cm^{-1}.)[29] and M(I) complexes ($Fe(OEPone)^{-}$: 1671 cm^{-1}. $Co(OEPone)^{-}$: 1674 cm^{-1}.)[41,42] were not significant.

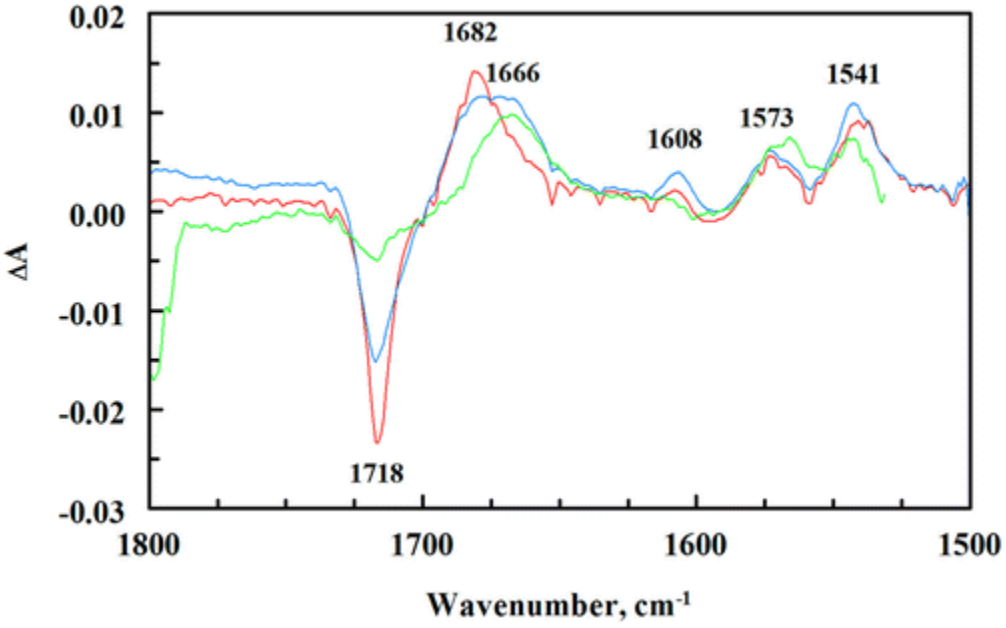

Figure 6. Difference FTIR spectra for the reduction at the first redox couple of Ni(OEPone) in THF/0.10 M TBAP (red line), in THF/33% $AmNTf_2$ (blue line), and in pure $AmNTf_2$ (green).

The FTIR spectroelectrochemical experiment was then repeated in a 33%$AmNTf_2$/THF solution. In the presence of the RTIL, there was a small but measurable shift in the ν_{CO} band for Ni(OEPone) from 1717 to 1715 cm^{-1}, consistent with what was observed in pure $AmNTf_2$. Upon reduction, though, the ν_{CO} was significantly broadened indicating that there were probably two ν_{CO} bands for $Ni(OEPone)^{-}$ (blue line, Figure 6). On the other hand, the bands at 1608 and 1573 cm^{-1} were unaffected, but there was a small upshift in the 1541 cm^{-1} band. The difference spectrum for the ν_{CO} band was analyzed using GRAMS to deconvolute the bands. Because of the small shift in the ν_{CO} for Ni(OEPone), there may have also been two bands for the starting

Analytical Chemistry, Vol 87, No. 24 (November 10, 2015): pg. 12245-12253. DOI.

material. The deconvolution of the ν_{CO} bands is shown in Figure 7 for 33%$AmNTf_2$/THF. The results were consistent with two bands for $Ni(OEPone)^-$ at 1682 and 1666 cm^{-1}. Similarly, two bands were observed for Ni(OEPone) with the 1718 cm^{-1} being the dominant species, but a small difference band at 1707 cm^{-1} was observed (it is not unusual for the difference bands to be shifted from the absorbance spectrum when the bands are close together). From the deconvolution, the difference peak areas were nearly equal for the 1682 and 1666 cm^{-1} bands. The experiment was then repeated at different concentrations of the RTIL. As the %RTIL increased, the band at 1666 cm^{-1} grew at the expense of the 1682 cm^{-1} band. The difference spectrum in pure $AmNTf_2$ is shown as the green trace in Figure 6. The bands at 1682 and 1608 cm^{-1} disappeared and only the 1666 cm^{-1} band remained. The two bands at 1666 and 1682 cm^{-1} indicate that $Ni(OEPone)^-$ experienced two different types of solvation environments in the mixed RTIL/THF solutions. The 1682 cm^{-1} band was attributed to the THF domain, whereas the 1666 cm^{-1} band was assigned to the RTIL domain.

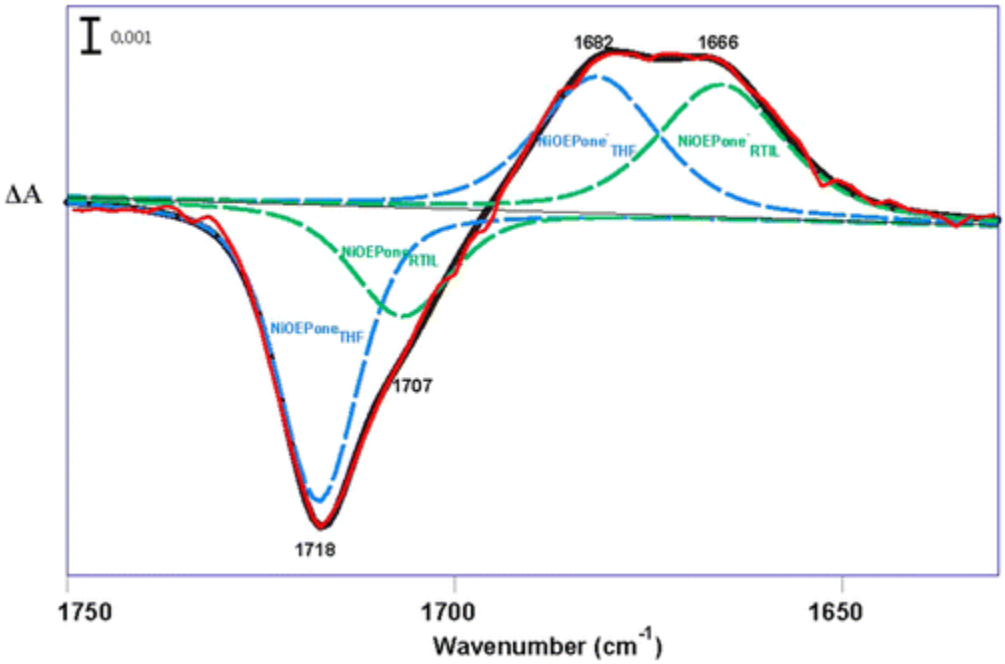

Figure 7. Deconvolution of the difference spectra for the reduction of Ni(OEPone) in THF/33% $AmNTf_2$. Red line: experimental difference spectrum. Black line: calculated difference spectrum. Green lines: bands for Ni(OEPone) species in $AmNTf_2$. Blue lines: bands for Ni(OEPone) species in THF.

Analytical Chemistry, Vol 87, No. 24 (November 10, 2015): pg. 12245-12253. DOI.

DFT calculations were carried out for the Ni(OEPone)$^-$ species. The spin density plot predicted a π-anion radical structure for the Ni(OEPone)$^-$ species (Figure S4). The predicted value for the ν_{CO} band was found to be 1652 cm^{-1}, compared to the experimental value of 1666 cm^{-1}. Additional bands were observed (calculated in parentheses) at 1573 cm^{-1} (1574) and 1541 cm^{-1} (1551), and no band was predicted at 1608 cm^{-1}. In general, the m06 functional favors delocalization of the charge, and hence the formation of a π-anion radical species.

The distribution of Ni(OEPone) and Ni(OEPone)$^-$ between the THF and RTIL nanodomains can be estimated from the difference peaks. By integrating the area under the difference bands shown in Figure 6, the distribution constant can be calculated assuming that there are two nanophases: RTIL nanodomain and the THF nanodomains. The distribution constant, D, is equal to

$$D = \frac{M_{RTIL}}{M_{THF}} = \frac{\#mol_{RTIL}/V_{RTIL}}{\#mol_{THF}/V_{THF}} \quad (3)$$

where M = molarity of Ni(OEPone)$^-$ in the RTIL or THF phase, #mol is the number of moles of Ni(OEPone)$^-$ in the RTIL or THF phase, V_{RTIL} is the total volume of added RTIL and V_{THF} is the total volume of added THF. If $mol_{total} = \#mol_{RTIL} + \#mol_{THF}$, then, dividing the top and bottom of the right-hand side by mol_{total}, we obtain

$$D = \frac{(\#mol_{RTIL}/mol_{total})/V_{RTIL}}{(\#mol_{THF}/mol_{total})/V_{THF}} = \frac{X_{Ni,RTIL}V_{THF}}{X_{Ni,THF}V_{RTIL}} = \frac{X_{Ni,RTIL}V_{THF}}{(1 - X_{Ni,RTIL})V_{RTIL}} \quad (4)$$

where $X_{Ni,RTIL}$ is the mole fraction of Ni(OEPone)$^-$ in the RTIL phase and $X_{Ni,THF}$ is the mole fraction of Ni(OEPone)$^-$ in the THF phase. Rearranging this equation, we can obtain

$$\frac{V_{RTIL}}{X_{Ni,RTIL}} = V_{RTIL} + \frac{V_{THF}}{D} \quad (5)$$

For V_{THF} = 1.00 mL, eq 5 becomes

$$\frac{1}{X_{Ni,RTIL}} = V_{RTIL} + \frac{1}{D} = \frac{DV_{RTIL} + 1}{DV_{RTIL}} \quad (6)$$

A value of D = 2.8 was obtained from eq 6 (Figure S5). For Ni(OEPone), the distribution into the RTIL layer was small, making the

Analytical Chemistry, Vol 87, No. 24 (November 10, 2015): pg. 12245-12253. DOI.

calculation more difficult, but, for the highest concentration of RTIL, a value of D = 0.5 can be estimated. This is consistent to the expectation that the anionic species are more soluble than the neutral within the RTIL domain.

The experiment was then repeated with the oxidation of Ni(OEPone) (Figure 8). As before, two bands were observed for Ni(OEPone) but only one band for Ni(OEPone)$^+$. This may be due to the fact that the ν_{CO} for Ni(OEPone)$^+$ was the same in both THF and the RTIL, or that Ni(OEPone)$^+$ favors the THF nanodomains over the RTIL nanodomains. Given that the neutral, Ni(OEPone), shifted in going from THF to the RTIL, the second explanation is the most likely one. In addition, the minimal change in the $\Delta E_{12,ox}°$ with the addition of the RTIL indicates a weaker interaction between the cations and the RTIL.

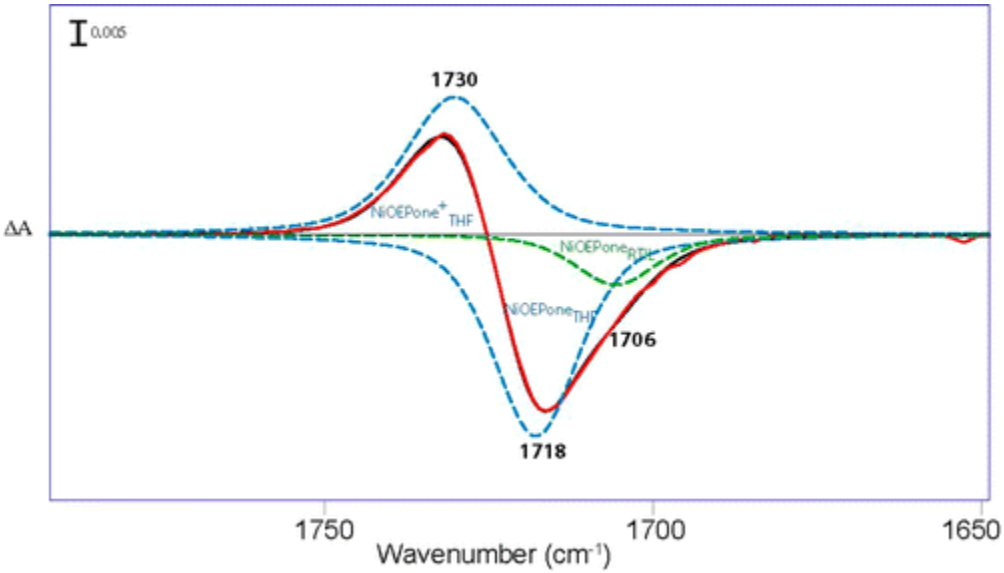

Figure 8. Deconvolution of the difference spectra for the oxidation of Ni(OEPone) in THF/33% $AmNTf_2$. Red line: experimental difference spectrum. Black line: calculated difference spectrum. Green lines: bands for Ni(OEPone) species in $AmNTf_2$. Blue lines: bands for Ni(OEPone) species in THF.

A comparison of the $E°$ shifts for Ni(OEP) and Ni(OEPone) indicates the complexity of the interactions between the RTIL and charged substrates. The shifts in the $E_1°$ and $E_2°$ values for Ni(OEP) can be understood mostly on the basis of electrostatics. Significantly larger shifts were observed for the dianion (Ni(OEP)$^{2-}$) than for the monoanion (Ni(OEP)$^-$). On the other hand, the shifts in the $E_1°$ and $E_2°$

Analytical Chemistry, Vol 87, No. 24 (November 10, 2015): pg. 12245-12253. DOI.

values for Ni(OEPone) were more complex, and cannot be explained simply on the basis of the overall charge. The FTIR spectroelectrochemical data clearly showed a strong interaction between $Ni(OEPone)^-$ and the RTIL phase, causing a significant downshift in the ν_{CO} band. The visible spectra (broad weak Soret band) already showed that there was significant ring delocalization of the negative charge in $Ni(OEPone)^-$, indicating that the $Ni(OEPone)^-$ complex is more like a π-radical anion than a Ni(I) complex. The large shift in the $E_1°$ value in THF between Ni(OEP) and Ni(OEPone) is consistent with this result. The weakening of the ν_{CO} bond in the presence of the RTIL shows that the RTIL environment favors additional electron density on the CO group. Previous DFT calculations for other metalloporphinones have shown that the HOMO orbital is antibonding at the C═O moiety.[29,41,42] In addition, the interaction of $Ni(OEPone)^-$ with the RTIL nanodomains shifts more electron density to the C═O moiety.

This downshift in the ν_{CO} band cannot be simply the effect of ion pairing. The Am^+ cation is very similar in size and ion pairing ability to TBA^+, which was present in the THF solution. If it was ion pairing alone, the band at 1666 cm^{-1} should have been observed in the THF/TBAP solution. The presence of RTIL nanodomains (aggregates) allows for a more powerful interaction between the substrate and the ions of the RTIL. The electronic structure of $Ni(P)^-$ species is a sensitive function of the nature of the porphyrin. This has been examined by Ryeng et al. using DFT for nickel hydroporphines.[43] The difference between Ni(I) and the π-radical anion is not large, and is dependent upon the environment and flexibility of the porphyrin ring. Both Ni(I) and π-radical anion species have been observed.[15,44]

The $E°$ value shifts for Ni(OEP)/Ni(OEPone) reported in this work, along with previously reported shifts for dinitrobenzene (DNB) is indicative of the charge/structure effects on the interaction of anions with RTILs. For Ni(OEP) and DNB, the most significant shifts were observed for the $E_2°$ values. On the other hand, the $E_1°$ value was most affected for Ni(OEPone). For $DNB^{-\bullet}$, the charge was significantly delocalized over the entire molecule, minimizing the interactions between the RTIL and the substrate. A similar effect probably occurred for $Ni(OEP)^-$ due to backbonding of the Ni(I) electron density to the porphyrin ring. As a result, the electrostatic interaction between the

Analytical Chemistry, Vol 87, No. 24 (November 10, 2015): pg. 12245-12253. DOI.

anion and the RTIL was not strong. On the other hand, for $Ni(OEPone)^{-}$, the electron density was already significantly delocalized on the ring, and the presence of the RTIL concentrated that electron density on the polar C═O moiety, allowing for a significant electrostatic interaction between the RTIL and $Ni(OEPone)^{-}$. This interaction was probably not significantly strengthened with the formation of the dianion, $Ni(OEPone)^{2-}$ (presumed to be a Ni(I) π-radical anion structure) because the Ni(OEPone) species was already incorporated into the RTIL nanodomain. The formation of a Ni(I) complex would not significantly increase the interaction with the RTIL. With the formation of DNB^{2-} and $Ni(OEP)^{2-}$, the mostly planar complex would be able to incorporate easily into the RTIL domain, leading to significant potential shifts in $E_2°$ values.

Although the reduction potentials can be strongly affected by the presence of RTILs, the oxidation potentials were not. Most RTILs consist of large cations with small anions. RTILs are formed because of the weak electrostatic interaction between the cations and anions, mostly caused by steric effects. Otherwise, the salts would be solids if the interactions were strong. Large anions such as $Ni(OEP)^{-/2-}$ can be readily solvated by the large RTIL cations without introducing electrostatic repulsion between the cations of the RTILs. On the other hand, the cations such as $Ni(OEP)^{+/2+}$ are not incorporated well into the RTIL nanodomains because of cation–cation repulsion in the RTIL nanodomains. This is clearly seen in the FTIR. The neutral Ni(OEPone) species can interact to some extent with the RTIL nanodomains, though equilibrium favors their presence in the THF nanodomains. On the other hand, there is no evidence of significant interaction between $Ni(OEPone)^{+}$ and the RTIL as only one ν_{CO} band was observed in the oxidized species.

Finally, the diffusion of Ni(OEP) in the mixed solvent is controlled mostly by the %THF in the solution rather than the solution viscosity. The results, which indicate a linear relationship between the diffusion coefficient and %RTIL, are only empirical at this point. Work is in progress to develop a theoretical basis for this observation. At this time though, the results are consistent with separate THF and RTIL nanodomains with the electroactive material diffusing through the THF domain. The diffusion coefficient does not follow the Stokes–Einstein

Analytical Chemistry, Vol 87, No. 24 (November 10, 2015): pg. 12245-12253. DOI.

relationship for molecular solvent rich solution, even though it is observed for pure molecular and RTIL solutions.

Conclusion

The results of the voltammetric and spectroscopic data were consistent with the formation of nanodomains in THF/RTIL mixtures. The exchange between the two nanodomains was slow enough to observe the two species using FTIR for Ni(OEPone) and $Ni(OEPone)^-$. The partitioning between the THF and RTIL domains is controlled by both electrostatic and electronic factors. RTILs preferentially solvate electrogenerated anions over electrogenerated cations. The large electrogenerated anions are able to interact strongly with the RTIL cation without increasing repulsion between the ions of the RTIL. Because the RTIL cation is larger than the RTIL anion, incorporation of the electrogenerated cations will cause significant cation–cation repulsion. In addition to the charge on the substrate, the formation of polar moieties within the substrates increases the interactions between the substrates and the RTIL. As a result, the RTIL can affect the distribution of electron density within the molecule, favoring additional electron density at polar sites that can attract the cation of the RTIL. By increasing the polarity of polar groups, the reactivity and reaction course could be changed. Indications of this switch in the reaction course was shown in the reduction of CO_2 in mixed acetonitrile/$EMImNTf_2$ solutions. The presence of $EMImNTf_2$ switched the reaction course from the oxalate anion to CO.[45] Work is continuing in our laboratory to investigate how the interaction of RTILs with anionic substrates in mixed solvents can be observed spectroscopically and their structural consequences. Finally, the diffusion of electroactive species in molecular solvent/RTIL mixtures occurs mostly within the molecular solvent domain. The RTIL will decrease the diffusion coefficient of the electroactive species, but not nearly as much as predicted by the Stokes–Einstein equation.

Supporting Information

The Supporting Information is available free of charge on the ACS Publications website at DOI: 10.1021/acs.analchem.5b03411.

Analytical Chemistry, Vol 87, No. 24 (November 10, 2015): pg. 12245-12253. DOI.

- Cyclic voltammetries, spectroelectrochemical oxidation, spectroelectrochemical reduction, spin density plot and plot of the reciprocal of the mole fraction (PDF).

The authors declare no competing financial interest.

Acknowledgment

We acknowledge the Schmitt Foundation for fellowship support of Abderrahman Atifi.

References

[1]Hapiot, P.; Lagrost, C. *Chem. Rev.* 2008, 108, 2238– 2264, DOI: 10.1021/cr0680686

[2]Fry, A. J. J. *Electroanal. Chem.* 2003, 546, 35– 39, DOI: 10.1016/S0022-0728(03)00143-8

[3]Atifi, A.; Ryan, M. D. *Anal. Chem*. 2014, 86, 6617– 6625, DOI: 10.1021/ac5012987

[4]Nikitina, V. A.; Nazmutdinov, R. R.; Tsirlina, G. A. J*. Phys. Chem. B* 2011, 115, 668– 677, DOI: 10.1021/jp1095807

[5]Nikitina, V. A.; Gruber, F.; Jansen, M.; Tsirlina, G. A. *Electrochim. Acta* 2013, 103, 243– 251, DOI: 10.1016/j.electacta.2013.04.069

[6]Consorti, C. S.; Suarez, P. A. Z.; de Souza, R. F.; Burrow, R. A.; Farrar, D. H.; Lough, A. J.; Loh, W.; Da Silva, L. H. M.; Dupont, J. *J. Phys. Chem. B* 2005, 109, 4341– 4349, DOI: 10.1021/jp0452709

[7]Li, W.; Zhang, Z.; Zhang, J.; Han, B.; Wang, B.; Hou, M.; Xie, Y. *Fluid Phase Equilib.* 2006, 248, 211– 216, DOI: 10.1016/j.fluid.2006.08.013

[8]Bagno, A.; Scorrano, G.; Stiz, S. *J. Am. Chem. Soc.* 1997, 119, 2299– 2300, DOI: 10.1021/ja963707n

[9]Rastrelli, F.; Saielli, G.; Bagno, A.; Wakisaka, A. *J. Phys. Chem. B* 2004, 108, 3479– 3487, DOI: 10.1021/jp037433j

[10]Shin, D. N.; Wijnen, J. W.; Engberts, J. B. F. N.; Wakisaka, A. *J. Phys. Chem. B* 2001, 105, 6759– 6762, DOI: 10.1021/jp0111517

[11]Bhat, M. A. *Electrochim. Acta* 2012, 81, 275– 282, DOI: 10.1016/j.electacta.2012.07.059

[12]Syroeshkin, M. A.; Mendkovich, A. S.; Mikhal'chenko, L. V.; Gul'tyai, V. P. *Russ. Chem. Bull.* 2009, 58, 1688– 1693, DOI: 10.1007/s11172-009-0233-x

[13]Lagrost, C.; Carrie, D.; Vaultier, M.; Hapiot, P. *J. Phys. Chem. A* 2003, 107, 745– 752, DOI: 10.1021/jp026907w

[14]Kadish, K. M.; Franzen, M. M.; Han, B. C.; Araullo-McAdams, C.; Sazou, D. *J. Am. Chem. Soc.* 1991, 113, 512– 517, DOI: 10.1021/ja00002a019

[15]Kadish, K. M.; Franzen, M. M.; Han, B. C.; Araullomcadams, C.; Sazou, D. *Inorg. Chem.* 1992, 31, 4399– 4403, DOI: 10.1021/ic00047a030

[16]Lexa, D.; Momenteau, M.; Mispelter, J.; Savéant, J.-M. *Inorg. Chem.* 1989, 28, 30– 35, DOI: 10.1021/ic00300a009

[17]Stolzenberg, A. M.; Glazer, P. A.; Foxman, B. M. *Inorg. Chem.* 1986, 25, 983– 991, DOI: 10.1021/ic00227a020

[18]Connick, P. A.; Macor, K. A. *Inorg. Chem.* 1991, 30, 4654– 4663, DOI: 10.1021/ic00024a038

[19]Nahor, G. S.; Neta, P.; Hambright, P.; Robinson, L. R.; Harriman, A. *J. Phys. Chem.* 1990, 94, 6659– 6663, DOI: 10.1021/j100380a026

[20]Czernuszewicz, R. S.; Macor, K. A.; Li, X. Y.; Kincaid, J. R.; Spiro, T. G. *J. Am. Chem. Soc.* 1989, 111, 3860– 3869, DOI: 10.1021/ja00193a017

[21]Fuhrhop, J. H.; Mauzerall, D. *J. Am. Chem. Soc.* 1969, 91, 4174– 4181, DOI: 10.1021/ja01043a027

[22]Stolzenberg, A. M.; Stershic, M. T. *Inorg. Chem.* 1988, 27, 1614– 1620, DOI: 10.1021/ic00282a021

[23]Scheidt, W. R.; Buentello, K. E.; Ehlinger, N.; Cinquantini, A.; Fontani, M.; Laschi, F. *Inorg. Chim. Acta* 2008, 361, 1722– 1727, DOI: 10.1016/j.ica.2006.12.028

[24]Scheidt, W. R.; Cheng, B.; Haller, K. J.; Mislankar, A.; Rae, A. D.; Reddy, K. V.; Song, H.; Orosz, R. D.; Reed, C. A.; Cukiernik, F.; Marchon, J.-C. *J. Am. Chem. Soc.* 1993, 115, 1181– 1183, DOI: 10.1021/ja00056a072

[25]Fajer, J.; Borg, D. C.; Forman, A.; Dolphin, D.; Felton, R. H. *J. Am. Chem. Soc.* 1970, 92, 3451– 3459, DOI: 10.1021/ja00714a038

[26]Lagunas, M. C.; Silvester, D. S.; Aldous, L.; Compton, R. G. *Electroanalysis* 2006, 18, 2263– 2268, DOI: 10.1002/elan.200603645

[27]Adamiak, W.; Shul, G.; Rozniecka, E.; Satoh, M.; Chen, J.; Opallo, M. *Electroanalysis* 2011, 23, 1921– 1927, DOI: 10.1002/elan.201100188

[28]Compton, D. L.; Laszlo, J. A. *J. Electroanal. Chem.* 2002, 520, 71– 78, DOI: 10.1016/S0022-0728(01)00747-1

[29]Tutunea, F.; Atifi, A.; Ryan, M. D. *J. Electroanal. Chem.* 2015, 744, 17– 24, DOI: 10.1016/j.jelechem.2015.02.024

[30]Schmeisser, M.; Illner, P.; Puchta, R.; Zahl, A.; van Eldik, R. *Chem. - Eur. J.* 2012, 18, 10969– 10982S10969-1, DOI: 10.1002/chem.201200584

[31]Frisch, M. J.; Trucks, G. W.; Schlegel, H. B.; Scuseria, G. E.; Robb, M. A.; Cheeseman, J. R.; Scalmani, G.; Barone, B.; Mennucci, B.; Petersson, G. A.; Natatsuji, H.; Caricota, M.; Li, X.; Hratchian, H. P.; Izmaylov, A. F.; Bloino, J.; Zheng, G.; Sonnenberg, J. L.; Hada, M.; Ehara, M.; Toyota, K.; Fukuda, R.; Hasegawa, J.; Ishida, M.; Nakajima, T.; Honda, Y.; Kitao, O.; Nakai, H.; Vreven, T.; Montgomery, J. A., Jr.; Peralta, J. E.; Ogliaro, F.; Bearpark, M.; Heyd, J. J.; Brothers, E.; Kudin, K. N.; Staroverov, V. N.; Kobayashi, R.; Normand, J.;

Raghavachari, K.; Rendell, A.; Burant, J. C.; Iyengar, S. S.; Tomasi, J.; Cossi, M.; Rega, N.; Millam, N. J.; Klene, M.; Knox, J. E.; Cross, J. B.; Bakken, V.; Adamo, C.; Jaramillo, J.; Gomperts, R.; Stratmann, R. E.; Yazyev, O.; Austin, A. J.; Cammi, R.; Pomelli, C.; Ochterski, J. W.; Martin, R. L.; Morokuma, K.; Zakrzewski, V. G.; Voth, G. A.; Salvador, P.; Dannenberg, J. J.; Dapprich, S.; Daniels, A. D.; Farkas, Ö.; Foresman, J. B.; Ortiz, J. V.; Cioslowski, J.; Fox, D. J. Gaussian 09, Revision D.01, Gaussian, Inc.: Wallingford,CT, 2009.

[32]Wachters, A. J. H. J. Chem. Phys. 1970, 52, 1033– 1036, DOI: 10.1063/1.1673095

[33]Zhao, C.; Bond, A. M.; Lu, X. Anal. Chem. 2012, 84, 2784– 2791, DOI: 10.1021/ac2031173

[34]Stolzenberg, A. M.; Stershic, M. T. J. Am. Chem. Soc. 1988, 110, 6391– 6402, DOI: 10.1021/ja00227a020

[35]Li, X.-Y.; Czernuszewicz, R. S.; Kincaid, J. R.; Spiro, T. G. J. Am. Chem. Soc. 1989, 111, 7012– 7023, DOI: 10.1021/ja00200a018

[36]Rogers, E. I.; Silvester, D. S.; Poole, D. L.; Aldous, L.; Hardacre, C.; Compton, R. G. J. Phys. Chem. C 2008, 112, 2729– 2735, DOI: 10.1021/jp710134e

[37]Lagunas, M. C.; Pitner, W. R.; van den Berg, J.-A.; Seddon, K. R. ACS Symp. Ser. 2003, 856, 421– 438, DOI: 10.1021/bk-2003-0856.ch034

[38]Long, J. S.; Silvester, D. S.; Barnes, A. S.; Rees, N. V.; Aldous, L.; Hardacre, C.; Compton, R. G. J. Phys. Chem. C 2008, 112, 6993– 7000, DOI: 10.1021/jp800235t

[39]Zhang, X.; Yang, H.; Bard, A. J. J. Am. Chem. Soc. 1987, 109, 1916– 1920, DOI: 10.1021/ja00241a005

[40]Clegg, A. D.; Rees, N. V.; Klymenko, O. V.; Coles, B. A.; Compton, R. G. J. Am. Chem. Soc. 2004, 126, 6185– 6192, DOI: 10.1021/ja040014v

[41]Tutunea, F.; Ryan, M. D. J. Electroanal. Chem. 2012, 670, 16– 22, DOI: 10.1016/j.jelechem.2012.01.027

[42]Wei, Z.; Ryan, M. D. Inorg. Chem. 2010, 49, 6948– 6954, DOI: 10.1021/ic100614h

[43]Ryeng, H.; Gonzalez, E.; Ghosh, A. J. Phys. Chem. B 2008, 112, 15158– 15173, DOI: 10.1021/jp805486b

[44]Campbell, C. J.; Rusling, J. F.; Brückner, C. J. Am. Chem. Soc. 2000, 122, 6679– 6685, DOI: 10.1021/ja000749+

[45]Sun, L.; Ramesha, G. K.; Kamat, P. V.; Brennecke, J. F. Langmuir 2014, 30, 6302– 6308, DOI: 10.1021/la5009076